EUROPEAN RESPIRATORY *journal*

FLAGSHIP SCIENTIFIC JOURNAL OF ERS

Early View

Original article

Intrapulmonary airway smooth muscle is hyperreactive with a distinct proteome in asthma

Gijs Ijpma, Linda Kachmar, Alice Panariti, Oleg S. Matusovsky, Dara Torgerson, Andrea Benedetti, Anne-Marie Lauzon

Please cite this article as: Ijpma G, Kachmar L, Panariti A, *et al*. Intrapulmonary airway smooth muscle is hyperreactive with a distinct proteome in asthma. *Eur Respir J* 2020; in press (https://doi.org/10.1183/13993003.02178-2019).

Title: Intrapulmonary airway smooth muscle is hyperreactive with a distinct proteome in asthma

Authors: Gijs IJpma[1,2]; Linda Kachmar[1,2]; Alice Panariti[1,2]; Oleg S. Matusovsky[3]; Dara Torgerson[2,4]; Andrea Benedetti[1,5,6]; Anne-Marie Lauzon[1,2*]

Affiliations:

[1]Department of Medicine, McGill University, Montreal, Quebec, Canada.

[2]Research Institute of the McGill University Health Centre, Meakins-Christie Laboratories, Montreal, Quebec, Canada.

[3]Department of Kinesiology and Physical Education, McGill University, Montreal, Quebec, Canada.

[4]McGill University and Génome Québec Innovation Centre, Montreal, Quebec, Canada

[5]Department of Epidemiology, Biostatistics & Occupational Health, McGill University, Montreal, Quebec, Canada.

[6]Respiratory Epidemiology and Clinical Research Unit, McGill University Health Centre, Montreal, Quebec, Canada.

[*]**Corresponding Author:** Anne-Marie Lauzon, 1001 Decarie Blvd. EM3.2236, Montreal, QC, H4A3J1, Canada, 514-9341934x76176, anne-marie.lauzon@mcgill.ca

Take-Home message: Intrapulmonary, but not tracheal, airway smooth muscle is hyperreactive in asthma, together with pro-contractile changes in the airway smooth muscle proteome. Several proteins were identified that could be targeted for treatment of the hyperreactivity.

Keywords: Airway smooth muscle mechanics, asthma, proteomics, airway remodeling

Abstract:

Constriction of airways during asthmatic exacerbation is the result of airway smooth muscle (ASM) contraction. Although it is generally accepted that ASM is hypercontractile in asthma, this has not been unambiguously demonstrated. Whether airway hyperresponsiveness is the result of increased ASM mass alone or also increased contractile force generation per unit of muscle directly determines the potential avenues for treatment.

To assess whether ASM is hypercontractile we performed a series of mechanics measurements on isolated ASM from intrapulmonary airways and trachealis from human lungs. We analyzed ASM and whole airway proteome to verify if proteomic shifts contribute to changes in ASM properties.

We report an increase in isolated ASM contractile stress and stiffness specific to asthmatic human intrapulmonary bronchi, the site of increased airway resistance in asthma. Other contractile parameters were not altered. Principal component analysis of unbiased mass spectrometry data showed clear clustering of asthmatic subjects with respect to ASM specific proteins. The whole airway proteome showed upregulation of structural proteins. We did not find any evidence for a difference in the regulation of myosin activity in the asthmatic ASM.

In conclusion, we showed that ASM is indeed hyperreactive at the level of intrapulmonary airways in asthma. We identified several proteins that are upregulated in asthma that could contribute to hyperreactivity. Our data also suggest enhanced force transmission associated with enrichment of structural proteins in the whole airway. These findings may lead to novel directions for treatment development in asthma.

Introduction

Asthma, a common chronic disease affecting over 300 million people worldwide [1], is characterized by exaggerated constriction of the airways, i.e. airway hyperresponsiveness (AHR), in response to environmental stimuli. The causes of asthma are still unknown and the mechanisms underlying excessive bronchoconstriction are poorly characterized. In particular, while the role of airway smooth muscle (ASM) in bronchoconstriction is undeniable, no study has unambiguously shown hypercontractility of asthmatic ASM. A major problem with previous measurements is that they were either performed on isolated trachealis ASM, a tissue that is clinically irrelevant for asthma studies, or whole intrapulmonary airway rings or strips without isolating the muscle per se. In developing novel treatments for asthma, understanding whether we're up against hypercontractile ASM will be an essential part of the puzzle.

We and others previously showed that the contractile properties of human trachealis and main bronchi smooth muscle are not intrinsically altered in asthma [2, 3], although Chin et al. did find a difference in the response to large length oscillations [3]. However, we subsequently showed that in the spontaneously occurring horse model of asthma, the intrapulmonary ASM, but not the trachea, exhibits a significant increase in the maximum rate of shortening (V_{max}) [4]. This increase was dependent on the time since the last steroid treatment, suggesting that it resulted from the inflammatory environment of the intrapulmonary ASM [5]. In human asthma, inflammation has been shown to progressively increase towards the periphery [6], which may result in site-specific ASM behaviour. Indeed, by exposing the rat trachealis smooth muscle to inflammatory cells, we were able to recreate the increased V_{max} observed in the horse intrapulmonary ASM [7]. Furthermore, subjects with asthma show, in response to a single dose of anti-inflammatory drugs, a rapid but transient reduction in AHR [8, 9]. While reduced mucous content and airway swelling likely contribute to this [10], our studies suggest that a transient change in the ASM mechanics may also contribute to the reduced AHR.

Thus, to assess whether intrapulmonary ASM itself exhibits greater contractility in asthma, we isolated intrapulmonary (3rd to 5th branching generation) and trachealis ASM strips from fresh transplant-grade lungs from subjects with asthma and controls and compared their contractile properties. We subsequently performed mass-spectrometry measurements on the intrapulmonary airways to investigate the observed contractility changes.

Materials and Methods

Procurement and tissue preparation

Fresh asthmatic and control transplant-grade lungs were procured by the International Institute for the Advancement of Medicine and the National Disease Research Interchange. The study was approved by the McGill University Health Center Research Ethic Board. Criteria for inclusion as asthmatic were based on either existing medical records of asthma diagnosis, where available, or on next-of-kin reporting of an asthma diagnosis. Detailed preparation and transport protocols are described in SI Materials and Methods. Demographics and donor clinical detail summaries are shown in Table 1 with further details in Table S1.

					Mechanics (#IB-#T)				
	Subjects	**Age**	**BMI**	**Sex F/M**	**MCh**	**Iso**	**Vmax**	**Stiffness**	**Proteomics**
Asthma	12	39±4	29±2	5/7	5-8	4-5	7–9	6-7	6
Control	19	43±3	28±1	8/11	7-11	4-4	10-13	7-10	6

BMI=Body Mass Index. F=Female, M=Male. #IB-#T=number of subjects for intrapulmonary bronchi vs trachealis ASM. MCh=Methacholine dose-response, Iso=Isoproterenol dose-response, Vmax=maximal shortening velocity.

Table 1: Subject summary table and number of subjects assessed for each dataset

Upon arrival, lung lobes were separated, and the lower right and left lobes were placed in oxygenated Hank's Balanced Salt Solution (solution compositions in SI Materials and Methods) at 4°C for initial

dissection, while remaining lobes were used for other studies. Trachealis strips were isolated as previously described [2]. For ASM dissection details see SI Materials and Methods.

Mechanics Measurements

Muscle tissue strips were suspended in a horizontal tissue bath as previously described [2]. In cases where the in situ length could not be determined, the tissues were stretched to just above slack length [11]. Initial tests in our lab and other studies [12, 13] have shown that after an equilibration period with repeated contractions, smooth muscle contractile stress and Vmax (in current lengths per second) is independent of muscle length for a wide range of muscle lengths. The starting length will be referred to as the reference length (L_{ref}). Tissues were continuously flushed with Krebs solution at 1ml/min. For detailed description of equilibration and mechanics protocols, see SI Materials and Methods. In short, after a ~1h equilibration period we performed shortening velocity measurements using repeated isotonic contractions. A single MCh 10^{-5}M contraction with superimposed length oscillations, small enough to not affect the average contractile stress, was used to measure the viscoelastic properties of the tissues. Lastly, we performed MCh and isoproterenol dose-response measurements. ASM area derived from histology of the smooth muscle strip was used to calculate contractile stress from maximal force response values.

To reduce variability and in case of data rejection (see SI Rejection Criteria), we tested two intrapulmonary and two trachealis tissues for each lung. For details see Table S1.

Mass Spectrometry

Ultra-high Liquid Chromatography tandem Mass Spectrometry (uHPLC-MS/MS) was used on extracts from whole airways with parameters as described in SI Materials and Methods. Smooth muscle specific proteins were identified according to The Protein Atlas ([14] see SI Materials and Methods). Spectrum counts were normalized to total smooth muscle content using the sum of relative total exclusive spectrum counts for each smooth muscle protein.

Statistics

We used linear mixed models to estimate the difference for all mechanics measurements, with a random intercept to account for measurements taken from the same subject (n is number of subjects tested). Means, standard errors and p values were calculated from the mixed model regression analyses. Error bars are standard errors, geometric means are shown for EC_{50} data. Principal component analysis on proteomics data was performed in Matlab^{TM}. Significance of clustering of asthmatic patients and controls was tested by two-sided unpaired student's T-test on the scores along the first principal component. Tests for functional enrichment of proteins that varied in levels between asthmatic patients and controls were performed using the Database for Annotation, Visualization and Integrated Discovery (DAVID, version 7.6 [15]) with Bonferroni correction.

Results

Methacholine and Isoproterenol Dose-response

In the dose-response to MCh of isolated ASM strips from intrapulmonary airways, we observed a markedly increased maximal stress (σ_{max}, derived from dose-response curve fits to data, Fig. 1A) in asthmatic compared to control patients (109.6±20.1 vs 61.8±12.3kPa, p=0.04, Fig. 1B); this difference was not observed in trachealis ASM (94.9±21.6 vs 111.3±13.9kPa, p=0.46, Fig. 1B). A significant interaction ($p<0.05$) between disease state and site was found, indicating that the intrapulmonary and the trachealis ASM are affected differently by the disease. Asthmatic intrapulmonary ASM was found to be hyposensitive compared to controls (geometric means of half maximal effective concentration, EC_{50}: 5.6±0.21 vs 6.1±0.13 $-\log_{10}$ M MCh, p=0.02, Figs. 1C-D), whereas trachealis ASM did not show any significant difference (geometric means: 5.9±0.21 vs 6.2±0.14 $-\log_{10}$ M MCh, p=0.17).

We found no differences in the maximum relaxation to isoproterenol in intrapulmonary (asthma vs control: 61.3±13.5 vs. 66.2±9.6%, p=0.73) or tracheal ASM (asthma vs control: 58.2±11.4 vs. 59.5±7.5%, p=0.92, Fig. 1E-F) and no significant interaction (p=0.75). Likewise, we found no significant difference

in isoproterenol EC_{50} (geometric means asthma vs control intrapulmonary: 7.00±0.45 vs 7.09±0.32 $-\log_{10}$ M Iso, p=0.84, and asthma vs. control trachealis: 6.80±0.38 vs 6.72±0.24 $-\log_{10}$ M Iso, p=0.84, Fig. 1G) with no significant interaction between disease and location.

V_{max} and viscoelastic properties

To assess whether V_{max} is changed in human asthma and whether these changes are specific to different phases of contraction, we calculated V_{max} during electrical field stimulation (EFS) at 3 timepoints (5, 8 and 10s after the initiation of contraction) by extrapolating from force-velocity curves (Fig. 2A-C). We found no significant differences in V_{max} between asthma patients and controls and no time effect. We did find a significant effect of location on V_{max} (all intrapulmonary vs all trachea: 0.27±0.012 vs 0.38±0.029 L_{ref} s^{-1}, p<0.001, Fig. 2D).

To probe the viscoelastic properties of the muscle, we applied continuous small sinusoidal length oscillations for the duration of a single MCh contraction. Mean stress (Figs. 2 E-F) and stiffness (Figs.2 G-H) followed similar trajectories during contraction in trachealis and intrapulmonary ASM. A greater mean stress (142±105 KPa vs 52.7±15.1 KPa, p=0.047) and stiffness (10±5.9 MPa vs 3.7±1.4MPa, p=0.02) were observed in contracted asthmatic intrapulmonary ASM compared to control with no differences in trachealis ASM. No significant difference was found in the baseline, i.e. relaxed ASM stress and stiffness. Our data on the viscous properties of the tissues, as expressed by the dimensionless parameter hysteresivity (Figs. 2 I-J), showed no differences between trachealis or peripheral ASM from subjects with asthma or controls.

Protein expression.

To narrow down the possible causes of the hyperreactivity we performed unbiased mass-spectrometry on whole airway samples from the same location as our intrapulmonary mechanics samples. To assess smooth muscle specific changes, we included only those proteins that are specific to smooth muscle (42 out of 2272 detected proteins, Table S2 and figure S2A). The data heatmap of these proteins shows

separation of asthmatic and control subjects (Fig. 3A), except for subject 28 (control) and, to a lesser extent, subject 12 (asthma). As subject 28 may be a clinical outlier amongst controls because of the combination of high BMI, extensive home medication and potentially strong inflammation associated with autism [16], this subject was excluded from further analyses. Principal component analysis (PCA) on the proteomics data showed significant separation of asthma patients and controls along the first principal component (42% of variance explained, scores 1.19±1.34 vs. -1.43±0.45, p=0.0025, Fig 3B, Fig. S2B with subject 28 included). In PCA of total detected proteome of the airway samples (Fig. S3A), asthmatic and control subjects do not show significant separation along the two principal components with (Fig. S3B) or without subject 28 (Fig. 3D).

BMI, age and gender effects

We tested the correlation of maximum contractile stress, MCh dose-response EC_{50} and V_{max} with subject body mass index (BMI), age and gender. With Bonferroni correction for multiple correlation testing we found no significant partial correlations between the contractility parameters and each of the subject characteristics while controlling for the remaining two subject characteristics (Fig.4).

Discussion

Airway constriction in asthma has long been, mostly intuitively, associated with hyperreactivity (greater maximal response) and hypersensitivity (greater response at low doses) of ASM to contractile agonists. Previous attempts to verify this in isolated ASM tissues showed no differences between control and asthmatic trachealis [2, 3] or main bronchi ASM [2]. Earlier studies have looked at contractility in asthma of airway strips with epithelium [17-24], which is known to modulate the behaviour of ASM [25], or whole airway rings [22, 23], but no isolated intrapulmonary ASM tissues have been examined. Furthermore, most of these tissues were taken from lung resections from heavy smokers [17, 18, 22, 23] and many hours post-mortem [19-21]. Whole airway or airway strip contractile force was not changed in asthma [17-21], but increased when normalized for ASM cross-sectional area [22]. Increased isolated airway narrowing was also found in subjects with asthma [23]. In our study, we measured the contractility

of isolated intrapulmonary and extrapulmonary ASM. We showed that hyperreactivity of ASM is a feature of asthma after all, but it is limited to the site of asthmatic attacks, the intrapulmonary bronchi.

It is worth noting that the contractile stress in our intrapulmonary ASM from control subjects is lower compared to all tracheal ASM tissues and asthmatic intrapulmonary ASM tissues (Fig. 1B). Our contractile stress values correspond with published values from the same locations: ASM in healthy whole human airways [22] and trachealis ASM from healthy and asthmatic subjects [3]. This difference in healthy intrapulmonary ASM is possibly the result of a difference in function. In the healthy lung, the function of ASM in intrapulmonary bronchi is unknown, if there is a function at all [26], while trachealis ASM is activated during cough [27] to aid in expelling foreign objects. This difference in function may lead to suboptimal adaptation for force generation in healthy intrapulmonary ASM, which may be changed by inflammatory stimuli in asthma. Site specificity of the inflammatory environment may drive site specific changes in contractile properties. Several studies have shown a more severe inflammation progressively towards the periphery [5, 6, 28]. Our previous studies in animal models of asthma support the role of inflammatory cells and mediators in altering ASM contractile properties [4, 7] as well as their partial reversal induced by corticosteroids [4]. A recent study showed site specificity in Rho kinase 1 and 2 content in ASM, with higher concentrations in the asthmatic interpulmonary airways [29], potentially resulting from inflammation. Rho kinase inhibitors have been shown to reduce ASM contractile stress and resistance to length oscillations [30]. It was also recently shown that inflammation may directly modulate ASM contractility through upregulation and activation of the calcium sensing receptor [31]. The full effects of inflammatory cells on human ASM mechanical properties will require further investigation.

The paradoxical small change in MCh sensitivity, which mirrors the change we previously showed in main bronchi smooth muscle [2], is likely clinically irrelevant and may indicate that sensitivity is primarily caused by changes in the epithelial barrier function in asthma [32-34], which can modulate the sensitivity to contractile agonists by up to 3 orders of magnitude [25]. Human asthmatic bronchial strip preparations have previously shown either hyposensitivity to contractile agonists in asthmatic subjects

[19, 20], in agreement with the current study, or no change [21, 24]. Isoproterenol in three of these studies showed a decrease in sensitivity in both fatal [19, 21] and non-fatal [24] asthma, but a study on mostly mild cases found no change [20]. Our data, which are mostly from mild to moderate asthma subjects, seem to agree with [20].

Based on prior studies on horse intrapulmonary ASM [4] and co-culture of rat trachealis with T-cells [7] we had hypothesized that V_{max} in human intrapulmonary ASM would also be increased. However, we did not find any changes in V_{max} at either location in asthma, or any time dependence despite the large change in contractile stress over this time range. Future studies into time dependence of V_{max} in longer, agonist induced, contractions may yield different data. Alternatively, the lack of difference in V_{max} between control and asthma subjects may lie in the type of asthma. In the spontaneously occurring horse model of asthma [4], all horses are considered severe cases and their inflammation is primarily neutrophilic compared to eosinophilic in humans. These horses, as well as induced animal models of asthma, may have a much more persistent inflammatory environment in the lung than the mild to moderate asthmatics in the current study. In fact, we previously showed that rat trachealis exposed for only 24h to CD_4^+ T-cells have an increased V_{max} [7], suggesting that only during exacerbations the V_{max} is increased. Changes in stress may require challenges to occur over a much longer period, which may explain its absence in most animal models. Our data on the viscoelastic properties of the muscle indicate that these more persistent changes in the contractile stress do not affect the viscous properties of the muscle. If the viscous properties of cells are the result of frictional forces between proteins [35], then the lack of change in viscosity paired with an increase in contractile stress and stiffness points to increased force generation and/or force transmission without increased overall protein size and density.

Regardless of the mechanism responsible for the enhanced contractility found in asthmatic intra-pulmonary ASM, the proteomic signature of ASM gives a snapshot of the contractile apparatus and structural proteins that existing studies on body fluid proteomics [36], genome wide association studies [37], and RNA expression studies [38] cannot address. To date this is the first study to address, and find,

proteomic differences of ASM tissues between subjects with asthma and controls. Despite a relatively small sample size, a clear separation between asthmatic patients and controls was found in PCA, indicating that the relative protein composition of asthmatic ASM is indeed different from controls. Among the proteins that contribute most to the first principal component (Fig. 3C), increased zyxin (ZYX) and smoothelin (SMTN) have previously been implicated in asthma, ([39] and [38] respectively). Zyxin facilitates contractile recovery from stretch, such as occurs during deep inspiration, by repairing fragmented stress fibers [39]. Increased smoothelin has been associated with contractile, in contrast to proliferative, smooth muscle [40], while the inverse was found for the decreased Adipocyte Enhancer-binding Protein 1 (AEBP1) [41]. Increased synaptopodin-2 (SYNPO2) is linked to an increased filamentous to globular actin ratio [42].

PCA of the whole airway proteome (Fig. S3A) did not show clear clustering of asthmatic and control subjects with (Fig. S3B) or without subject 28 (Fig. 3D) . We tested for functional enrichment in proteins that varied between subjects with asthma and controls into DAVID [15] using total discovered proteins as background. All proteins (66) were increased in asthma (Fig. S3C). Cell component gene ontology (Table S4) showed enrichment of ‘cytoskeleton’ and its subset ‘actin cytoskeleton’ as well as ‘focal adhesions’ and ‘adherens junctions’. These results show that these structural proteins are increased relative to total airway wall protein content, which may reflect increased structural integrity and force transmission in the airway wall.

Asthma is fundamentally a mechanical disease with a poorly understood etiology, but which undoubtedly results in excessive airway constriction. Our study showed new evidence for the role of ASM in airway hyperresponsiveness, clearly demonstrating that airway origin matters when it comes to ASM contractility. We identified several proteins that require further study to understand their role in ASM hyperreactivity in asthma and may lead to avenues for treatment.

References

1. Papi A, Brightling C, Pedersen SE, Reddel HK. Asthma. *The Lancet* 2018: 391(10122): 783-800.
2. Ijpma G, Kachmar L, Matusovsky OS, Bates JHT, Benedetti A, Martin JG, Lauzon A-M. Human Trachealis and Main Bronchi Smooth Muscle Are Normoresponsive in Asthma. *Am J Respir Crit Care Med* 2015: 191(8): 884-893.
3. Chin LYM, Bossé Y, Pascoe C, Hackett TL, Seow CY, Paré PD. Mechanical properties of asthmatic airway smooth muscle. *Eur Respir J* 2012: 40(1): 45-54.
4. Matusovsky OS, Kachmar L, Ijpma G, Bates G, Zitouni N, Benedetti A, Lavoie J-P, Lauzon A-M. Peripheral Airway Smooth Muscle but not the Trachealis is Hypercontractile in an Equine Model of Asthma. *Am J Respir Cell Mol Biol* 2015: 54(5): 718-727.
5. Hamid Q, Song Y, Kotsimbos TC, Minshall E, Bai TR, Hegele RG, Hogg JC. Inflammation of small airways in asthma. *J Allergy Clin Immunol* 1997: 100(1): 44-51.
6. De Magalhães Simões S, Dos Santos MA, Da Silva Oliveira M, Fontes ES, Fernezlian S, Garippo AL, Castro I, Castro FFM, De Arruda Martins M, Saldiva PHN, Mauad T, Dolhnikoff M. Inflammatory cell mapping of the respiratory tract in fatal asthma. *Clin Exp Allergy* 2005: 35(5): 602-611.
7. Matusovsky OS, Nakada EM, Kachmar L, Fixman ED, Lauzon A-M. CD4+ T cells enhance the unloaded shortening velocity of airway smooth muscle by altering the contractile protein expression. *The Journal of Physiology* 2014: 592(Pt 14): 2999-3012.
8. Berge MVD, Luijk B, Bareille P, Dallow N, Postma DS, Lammers JWJ. Prolonged protection of the new inhaled corticosteroid fluticasone furoate against AMP hyperresponsiveness in patients with asthma. *Allergy* 2010: 65(12): 1531-1535.
9. Luijk B, Kempsford RD, Wright AM, Zanen P, Lammers J-WJ. Duration of effect of single-dose inhaled fluticasone propionate on AMP-induced bronchoconstriction. *Eur Respir J* 2004: 23(4): 559-564.
10. James A, Carroll N. Theoretic Effects of Mucus Gland Discharge on Airway Resistance in Asthma. *Chest* 1995: 107(3, Supplement): 110S.
11. Bates JHT, Bullimore SR, Politi AZ, Sneyd J, Anafi RC, Lauzon A-M. Transient oscillatory force-length behavior of activated airway smooth muscle. *Am J Physiol Lung Cell Mol Physiol* 2009: 297(2): L362-L372.
12. Pratusevich VR, Seow CY, Ford LE. Plasticity in canine airway smooth muscle. *J Gen Physiol* 1995: 105(1): 73-94.
13. Smolensky AV, Ford LE. The extensive length-force relationship of porcine airway smooth muscle. *J Appl Physiol* 2007: 102(5): 1906-1911.
14. Uhlén M, Fagerberg L, Hallström BM, Lindskog C, Oksvold P, Mardinoglu A, Sivertsson Å, Kampf C, Sjöstedt E, Asplund A, Olsson I, Edlund K, Lundberg E, Navani S, Szigyarto CA-K, Odeberg J, Djureinovic D, Takanen JO, Hober S, Alm T, Edqvist P-H, Berling H, Tegel H, Mulder J, Rockberg J, Nilsson P, Schwenk JM, Hamsten M, von Feilitzen K, Forsberg M, Persson L, Johansson F, Zwahlen M, von Heijne G, Nielsen J, Pontén F. Tissue-based map of the human proteome. *Science* 2015: 347(6220): 1260419.
15. Huang DW, Sherman BT, Lempicki RA. Systematic and integrative analysis of large gene lists using DAVID bioinformatics resources. *Nature Protocols* 2008: 4: 44.
16. Siniscalco D, Schultz S, Brigida AL, Antonucci N. Inflammation and Neuro-Immune Dysregulations in Autism Spectrum Disorders. *Pharmaceuticals (Basel)* 2018: 11(2): 56.
17. de Jongste JC, van Strik R, Bonta IL, Kerrebijn KF. Measurement of human small airway smooth muscle function in vitro with the bronchiolar strip preparation. *J Pharmacol Methods* 1985: 14(2): 111-118.
18. Ishida K, Pare PD, Hards J, Schellenberg RR. Mechanical properties of human bronchial smooth muscle in vitro. *J Appl Physiol* 1992: 73(4): 1481-1485.

19. Goldie RG, Spina D, Henry PJ, Lulich KM, Paterson JW. In vitro responsiveness of human asthmatic bronchus to carbachol, histamine, beta-adrenoceptor agonists and theophylline. *Br J Clin Pharmacol* 1986: 22(6): 669-676.
20. Whicker SD, Armour CL, Black JL. Responsiveness of bronchial smooth muscle from asthmatic patients to relaxant and contractile agonists. *Pulm Pharmacol* 1988: 1(1): 25-31.
21. Bai TR. Abnormalities in Airway Smooth Muscle in Fatal Asthma: A Comparison between Trachea and Bronchus. *Am J Respir Crit Care Med* 1991: 143(2): 441-443.
22. Opazo Saez A, Seow C, Paré P. Peripheral Airway Smooth Muscle Mechanics in Obstructive Airways Disease. *Am J Respir Crit Care Med* 2000: 161(3): 910-917.
23. Noble PB, Jones RL, Cairncross A, Elliot JG, Mitchell HW, James AL, McFawn PK. Airway narrowing and bronchodilation to deep inspiration in bronchial segments from subjects with and without reported asthma. *J Appl Physiol* 2013: 114(10): 1460-1471.
24. Cerrina J, Ladurie MLR, Labat C, Raffestin B, Bayol A, Brink C. Comparison of Human Bronchial Muscle Responses to Histamine in vivo with Histamine and Isoproterenol Agonists in vitro 1, 2. *American Review of Respiratory Disease* 1986: 134(1): 57-61.
25. Goldie RG, Papadimitriou JM, Paterson JW, Rigby PJ, Self HM, Spina D. Influence of the epithelium on responsiveness of guinea-pig isolated trachea to contractile and relaxant agonists. *Br J Pharmacol* 1986: 87(1): 5-14.
26. Mitzner W. Airway Smooth Muscle: The Appendix of the Lung. *Am J Respir Crit Care Med* 2004: 169(7): 787-790.
27. Sant'Ambrogio G, Widdicombe J. Reflexes from airway rapidly adapting receptors. *Respir Physiol* 2001: 125(1): 33-45.
28. Balzar S, Wenzel SE, Chu HW. Transbronchial biopsy as a tool to evaluate small airways in asthma. *Eur Respir J* 2002: 20(2): 254-259.
29. Wang L, Chitano P, Paré PD, Seow CY. Upregulation of smooth muscle Rho-kinase protein expression in human asthma. *Eur Respir J* 2019.
30. Lan B, Deng L, Donovan GM, Chin LYM, Syyong HT, Wang L, Zhang J, Pascoe CD, Norris BA, Liu JCY, Swyngedouw NE, Banaem SM, Paré PD, Seow CY. Force maintenance and myosin filament assembly regulated by Rho-kinase in airway smooth muscle. *American journal of physiology Lung cellular and molecular physiology* 2015: 308(1): L1-L10.
31. Yarova PL, Stewart AL, Sathish V, Britt RD, Thompson MA, P. Lowe AP, Freeman M, Aravamudan B, Kita H, Brennan SC, Schepelmann M, Davies T, Yung S, Cholisoh Z, Kidd EJ, Ford WR, Broadley KJ, Rietdorf K, Chang W, Bin Khayat ME, Ward DT, Corrigan CJ, T. Ward JP, Kemp PJ, Pabelick CM, Prakash YS, Riccardi D. Calcium-sensing receptor antagonists abrogate airway hyperresponsiveness and inflammation in allergic asthma. *Science Translational Medicine* 2015: 7(284): 284ra260-284ra260.
32. Flavahan NA, Aarhus LL, Rimele TJ, Vanhoutte PM. Respiratory epithelium inhibits bronchial smooth muscle tone. *J Appl Physiol* 1985: 58(3): 834-838.
33. Gon Y, Hashimoto S. Role of airway epithelial barrier dysfunction in pathogenesis of asthma. *Allergol Int* 2018: 67(1): 12-17.
34. Sparrow MP, Mitchell HW, Omari TI. The epithelial barrier and airway responsiveness. *Can J Physiol Pharmacol* 1995: 73(2): 180-190.
35. Fredberg JJ, Jones KA, Nathan M, Raboudi S, Prakash YS, Shore SA, Butler JP, Sieck GC. Friction in airway smooth muscle: mechanism, latch, and implications in asthma. *J Appl Physiol* 1996: 81(6): 2703-2712.
36. Terracciano R, Pelaia G, Preianò M, Savino R. Asthma and COPD proteomics: Current approaches and future directions. *PROTEOMICS – Clinical Applications* 2015: 9(1-2): 203-220.
37. Vicente CT, Revez JA, Ferreira MAR. Lessons from ten years of genome-wide association studies of asthma. *Clin Transl Immunology* 2017: 6(12): e165-e165.

38. Pascoe CD, Obeidat Me, Arsenault BA, Nie Y, Warner S, Stefanowicz D, Wadsworth SJ, Hirota JA, Jasemine Yang S, Dorscheid DR, Carlsten C, Hackett TL, Seow CY, Paré PD. Gene expression analysis in asthma using a targeted multiplex array. *BMC pulmonary medicine* 2017: 17(1): 189-189.
39. Rosner SR, Pascoe CD, Blankman E, Jensen CC, Krishnan R, James AL, Elliot JG, Green FH, Liu JC, Seow CY, Park J-A, Beckerle MC, Paré PD, Fredberg JJ, Smith MA. The actin regulator zyxin reinforces airway smooth muscle and accumulates in airways of fatal asthmatics. *PLOS ONE* 2017: 12(3): e0171728.
40. Beamish JA, He P, Kottke-Marchant K, Marchant RE. Molecular regulation of contractile smooth muscle cell phenotype: implications for vascular tissue engineering. *Tissue Eng Part B Rev* 2010: 16(5): 467-491.
41. Layne MD, Endege WO, Jain MK, Yet SF, Hsieh CM, Chin MT, Perrella MA, Blanar MA, Haber E, Lee ME. Aortic carboxypeptidase-like protein, a novel protein with discoidin and carboxypeptidase-like domains, is up-regulated during vascular smooth muscle cell differentiation. *J Biol Chem* 1998: 273(25): 15654-15660.
42. Turczyńska Karolina M, Swärd K, Hien Tran T, Wohlfahrt J, Mattisson Ingrid Y, Ekman M, Nilsson J, Sjögren J, Murugesan V, Hultgårdh-Nilsson A, Cidad P, Hellstrand P, Pérez-García MT, Albinsson S. Regulation of Smooth Muscle Dystrophin and Synaptopodin 2 Expression by Actin Polymerization and Vascular Injury. *Arteriosclerosis, Thrombosis, and Vascular Biology* 2015: 35(6): 1489-1497.

Acknowledgments: We thank the proteomics core facility of the Research Institute of the McGill University Health Centre for their help with acquiring the mass-spectrometry data. We also thank Dr. James G. Martin for assistance in developing recovery protocols for donor lungs and interpretation of medical data. **Funding**: National Heart, Lung and Blood Institute grant RO1-HL 103405-02, Canadian Institute for Health Research and the Costello Fund. The Meakins-Christie Laboratories (McGill University Health Center Research Institute) are supported in part by a center grant from the Fonds de la Recherche en Santé Respiratoire du Québec. **Author contributions**: GI: Conception and Design; Acquisition of Data; Analysis and Interpretation of Data; Drafting and Review of Manuscript; LK: Acquisition of Data; Article review; AP: Acquisition of Data; Analysis of Data; Article Review; OSM: Acquisition of Data; Article review; AB: Statistical Advice; Article Review; DT: Proteomics analysis advice; Article review; AML: Conception and Design; Analysis and Interpretation of Data; Drafting and review of Manuscript. **Competing interests**: The authors declare no competing interests. **Data and materials availability**: All analyzed data and materials associated with this study are in the paper, raw data are available upon request.

Figure Legends

Figure 1: Dose-responses to methacholine (MCh) and isoproterenol (Iso). Black lines: controls, orange lines: subjects with asthma, solid lines: intrapulmonary, dashed lines: trachea. (A) Absolute dose-response curve to MCh (stress (σ) vs [MCh]). (B) Dot plot of maximum stress (σ_{max}). (C) Normalized MCh dose-response curves (normalized stress (σ) vs [MCh]). (D) Dot plot of sensitivity to MCh as expressed by EC_{50}, the dose at which 50% of maximal stress is generated. (E) Dose-response curve to Iso, with relaxation expressed as a percentage of the maximal contractile stress. (F) Dot plot of maximum relaxation. (G) Dot plot of sensitivity to Iso as expressed by EC_{50}.T: trachea, IP: intrapulmonary. * indicates $p<0.05$.

Figure 2: Force-velocity curves during Electrical Field Stimulation (EFS) and stress, stiffness and hysteresivity during MCh contraction. Black lines: controls, orange lines: subjects with asthma, solid lines intrapulmonary, dashed lines trachea. (A) Force-Velocity curves at 5 s into an EFS. (B) Force-Velocity curves at 8 s into an EFS. (C) Force-Velocity curves at 10 s into an EFS. (D) Maximal shortening velocity (V_{max}), from A-C. (E) and (F) mean stress (G) and (H) stiffness normalized to length (I) and (J) hysteresivity obtained by length oscillations during MCh stimulation as a function of time. Light gray and orange areas: 95% confidence interval.

Figure 3: Proteomics analysis from airways of asthmatic and control subjects. A) Heatmap of relative protein exclusive spectrum counts (left) with averaged normalized exclusive spectrum counts across all subjects for each protein (right). B) Plot of the first 2 principal components for all subjects except the clinical outlier #28 for smooth muscle specific proteins only. Black open circles are control subjects and red open circles are asthmatic subjects. C) Contribution of each protein to the first two principal components for smooth muscle specific proteins only. D) Plot of the first 2 principal components for all subjects except the clinical outlier #28 for whole airway proteins. Black open circles are control subjects and red open circles are asthmatic subjects.

Figure 4: Correlations of body mass index (BMI), age and sex for three contractility parameters, maximal stress (σ_{max}), MCh EC_{50} dose, and maximal shortening velocity (Vmax).

Figure 1

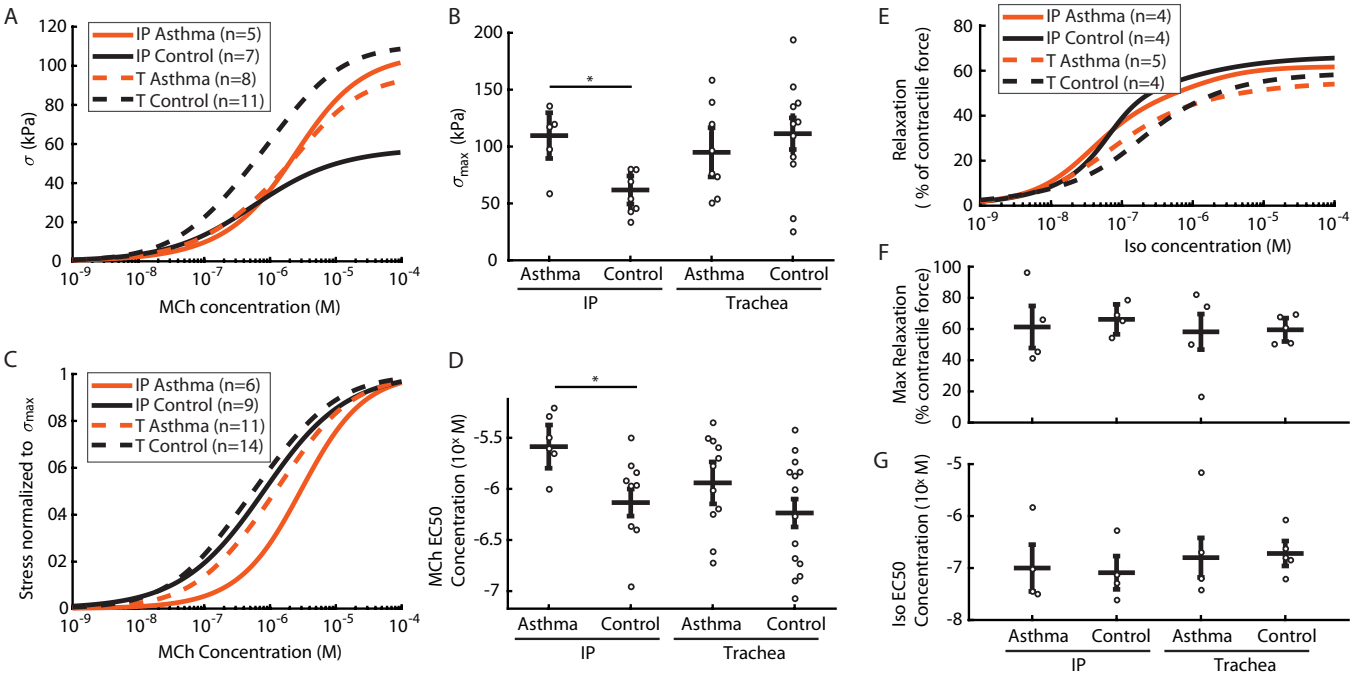
A
IP Asthma (n=5)
IP Control (n=7)
T Asthma (n=8)
T Control (n=11)
σ (kPa)
MCh concentration (M)
B
σmax (kPa)
Asthma
Control
Asthma
Control
IP
Trachea
C
IP Asthma (n=6)
IP Control (n=9)
T Asthma (n=11)
T Control (n=14)
Stress normalized to σmax
MCh Concentration (M)
D
MCh EC50 Concentration (10x M)
Asthma
Control
Asthma
Control
IP
Trachea
E
IP Asthma (n=4)
IP Control (n=4)
T Asthma (n=5)
T Control (n=4)
Relaxation (% of contractile force)
Iso concentration (M)
F
Max Relaxation (% contractile force)
G
Iso EC50 Concentration (10x M)
Asthma
Control
Asthma
Control
IP
Trachea

Figure 2

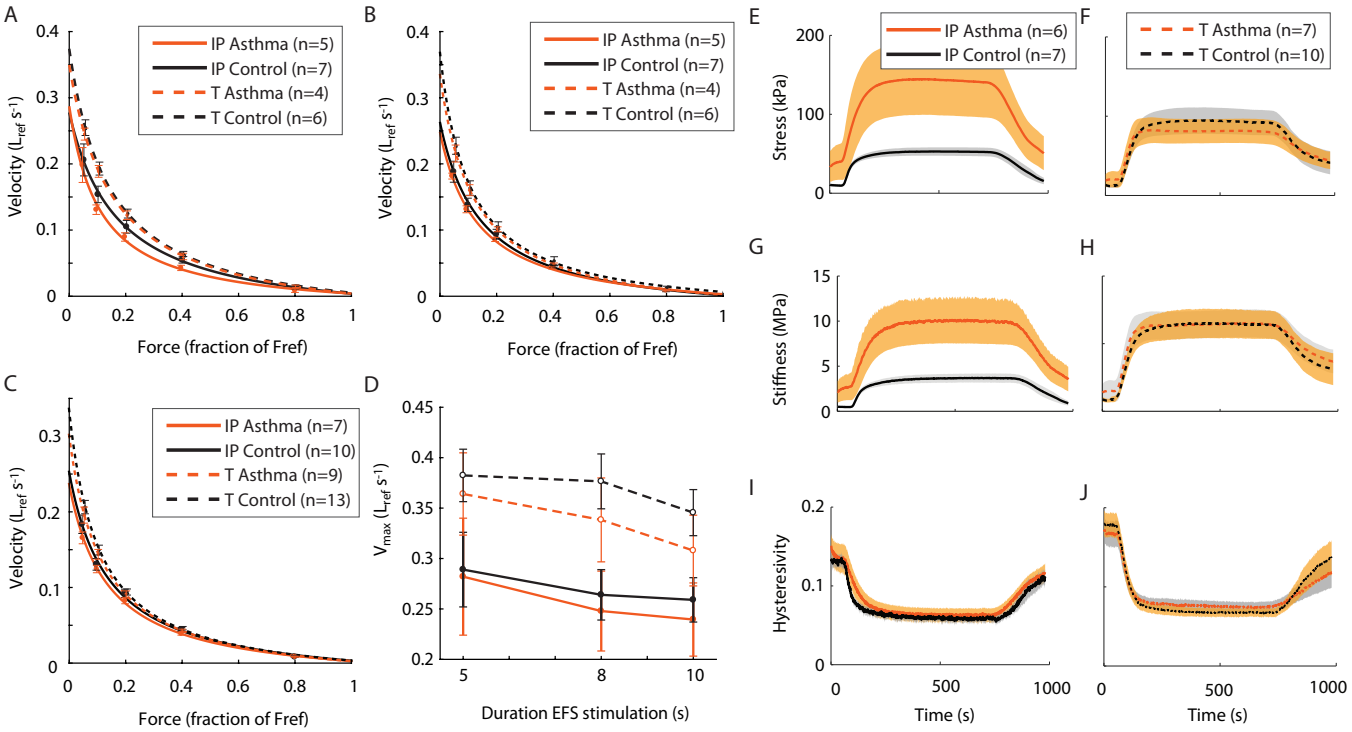
A
B
C
D
E
F
G
H
I
J
IP Asthma (n=5)
IP Control (n=7)
T Asthma (n=4)
T Control (n=6)
IP Asthma (n=7)
IP Control (n=10)
T Asthma (n=9)
T Control (n=13)
IP Asthma (n=6)
IP Control (n=7)
T Asthma (n=7)
T Control (n=10)
Velocity (Lref s-1)
Force (fraction of Fref)
Vmax (Lref s-1)
Duration EFS stimulation (s)
Stress (kPa)
Stiffness (MPa)
Hysteresivity
Time (s)

Figure 3

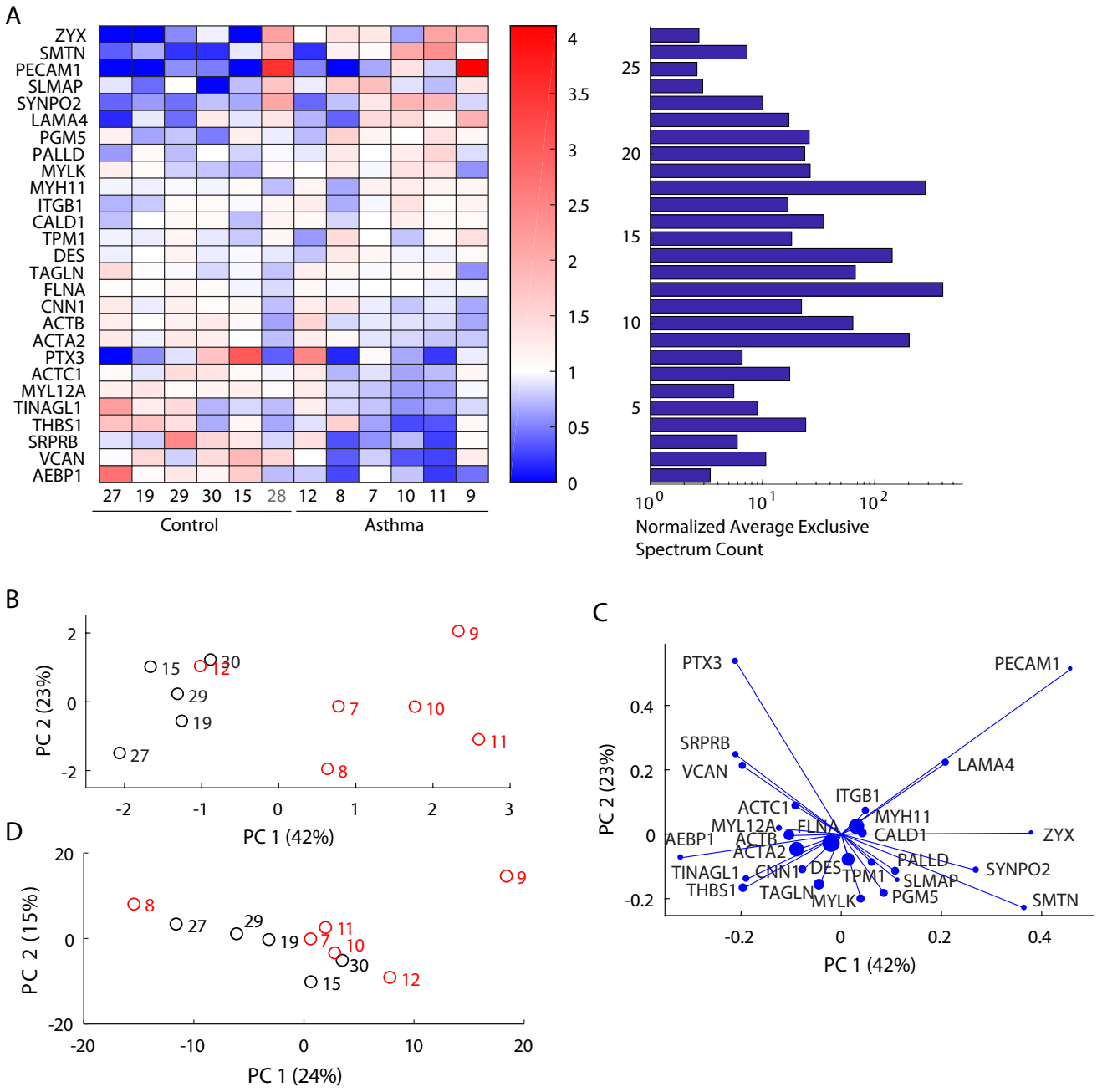
A
ZYX
SMTN
PECAM1
SLMAP
SYNPO2
LAMA4
PGM5
PALLD
MYLK
MYH11
ITGB1
CALD1
TPM1
DES
TAGLN
FLNA
CNN1
ACTB
ACTA2
PTX3
ACTC1
MYL12A
TINAGL1
THBS1
SRPRB
VCAN
AEBP1
27 19 29 30 15 28 12 8 7 10 11 9
Control
Asthma
4
3.5
3
2.5
2
1.5
1
0.5
0
25
20
15
10
5
10^0
10^1
10^2
Normalized Average Exclusive Spectrum Count
B
PC 2 (23%)
PC 1 (42%)
C
PC 2 (23%)
PC 1 (42%)
D
PC 2 (15%)
PC 1 (24%)

Figure 4

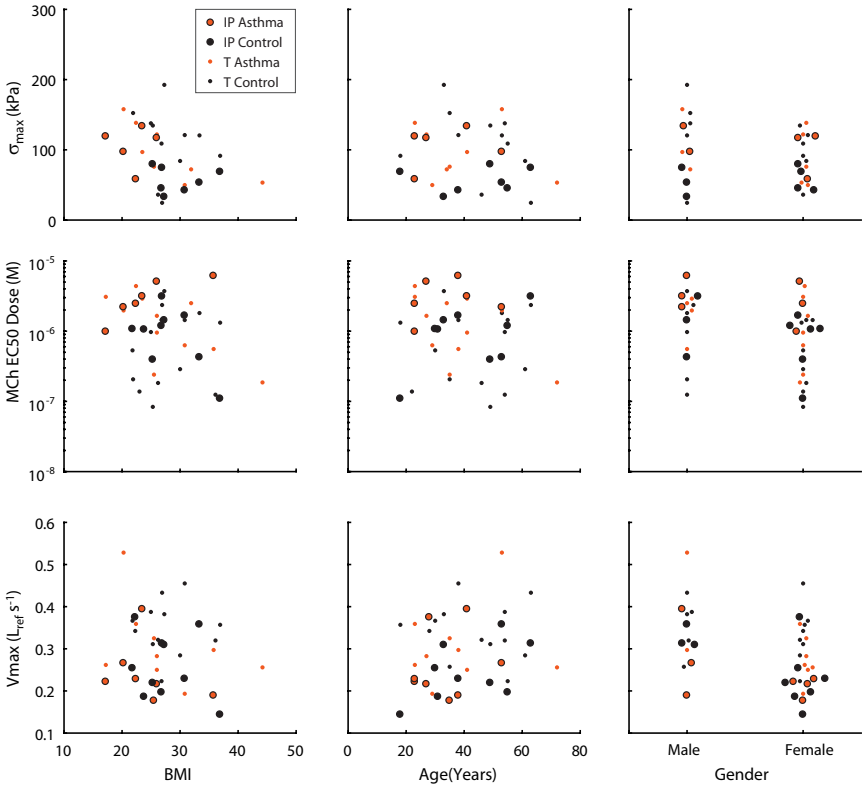
IP Asthma
IP Control
T Asthma
T Control
σ_{max} (kPa)
MCh EC50 Dose (M)
Vmax (L_{ref} s^{-1})
BMI
Age(Years)
Male
Female
Gender

Si Materials and methods

Solution composition

HBSS: composition in mM: 5.3 KCl, 0.44 KH_2PO_4, 137.9 NaCl, 0.336 Na_2PO_4, 2.33 $CaCl_2$, 0.79 $MgSO_4$, 10 glucose, 10 HEPES buffer, pH adjusted to 7.4 with NaOH)

Krebs: (composition in mM: 110 NaCl, 0.82 $MgSO_4$, 1.2 KH_2PO_4, 3.4 KCl, 25.7 $NaHCO_3$, 2.4mM $CaCl_2$, and 5.6 glucose, pH at 7.4, bubbled with 95/5% O_2/CO_2 gas mixture)

Ca2+ free Krebs, as normal Krebs without $CaCl_2$

Preparation, transport, and dissection

Lungs were recovered within 2 h after disconnection from the ventilator. Whole lung blood vessels were flushed with histidine-tryptophan-ketoglutarate (HTK) or University of Wisconsin (UW) solution after which the lungs were shipped in HTK or UW solution and arrived at our facility within 24 h of cross-clamp time.

Airway trees were dissected free from the parenchyma, taking care to minimize stress on the airways. Airway segments between the 3rd and 5th branching generations (2-6mm internal diameter) were dissected out. Segments were placed under a dissection microscope in Ca^{2+} free Krebs solution on ice for further dissection. Airway segments were cut open longitudinally, pinned down and epithelium was removed by stripping or cutting. ASM strips were carefully lifted out of the airway by cutting through the connective tissue layer. Muscle tissue strips were subsequently cleaned from any visible remaining connective tissue and aluminum foil clips were attached on either end of the tissue. ASM area of these dissected tissue strips, as determined from cross-sectional histology slides, averaged 0.0665 ± 0.0123mm^2.

Rejection criteria

As the availability of human lungs is unpredictable and certain measures were rejected because of technical difficulties, the actual sample size varied. To reduce variability, we tested two intrapulmonary and two trachealis tissues for each lung. Tissues that did not contract in response to EFS or MCh, or tissues that showed a >10% reduction in contractile force with repeated contractions, were rejected. Some tissues could not be tested for all protocols because of equipment malfunction, or because of post-hoc determined flaws in control parameter settings (inability to achieve a force control without overshoot). For details see Table S1.

Equilibration

Tissues were subsequently equilibrated using electrical field stimulations (EFS, 25 V/cm at 50Hz, 2ms pulse width for 10s) every 5min for 30min or until the resulting contractile force stabilized. This was followed by at least 5 contractions with MCh 10^{-5} M or 10^{-6} M MCh until a stable baseline and contractile force was achieved. 10^{-6} M MCh was used in earlier experiments where only trachealis muscle was tested, while 10^{-5} M MCh was found to be required for more recent experiments in which intrapulmonary muscle was also tested, as these tissues did not equilibrate well with 10^{-6} M MCh.

Dose response

Tissues were exposed to increasing concentrations of MCh from 10^{-8} M to 10^{-4} M every 100s (Fig. S1A). The peak force reached before each subsequent dose was taken as the force representative of that dose. To calculate stress, the force values were divided by the ASM cross-sectional area which was calculated as follows. Tissues were pinned down at L_{ref} on silicone strips and placed in 10% formalin for >24h, and fixed upright in paraffin to allow for cross-sectional cuts for histological analysis. 5µm thick slices were stained with alpha actin or Masson's Trichrome staining, each providing good contrast between ASM and non-muscle tissue. The ASM cross-section was traced and the area calculated. Both maximal stress and EC_{50}, the dose at which 50% of contractile stress was achieved, were calculated by fitting the data with a sigmoidal dose response curve.

After the tissue was exposed to the last MCh dose, it was exposed every 100s to increasing concentrations of isoproterenol (10^{-8} to 10^{-4}M) to measure its ability to relax (Fig. S1A). The minimum force achieved during each 100s interval was taken as the force representative of that dose. Both maximal relaxation and EC_{50}, the dose at which 50% of relaxation was achieved, were calculated by fitting the data with a sigmoidal dose response curve.

Shortening velocity

Shortening velocity measurements were performed at multiple time points to indirectly assess potential differences in cross-bridge cycling rates and their development during a contraction. Tissues were first shortened briefly by 25% of L_{ref} after which the reference zero force was measured (F_{zero}) to compensate for force drift in the force transducer. Subsequently the tissues were contracted with EFS for 5, 8 or 10s, immediately followed by a rapid 120ms force clamp (Fig. S1B, inset) to a force of 5, 7, 10, 20, 40 or 80% of the force just prior to the force clamp relative to F_{zero}, for a total of 21 individual EFS contractions. The slope of the length signal between 80 and 120ms of the force clamp duration was taken as the shortening velocity at this force clamp (Fig. S1B, inset). Force velocity plots were generated using these shortening velocity data and the post-hoc measured actual force clamp value between 80 and 120 ms. Force-Velocity curves were calculated by performing a perpendicular least squares fitting method of the classic hill curve ($V=b(F_0-F)/(a+F)$ (1).

Viscoelastic properties

To probe the viscoelastic properties of the muscle, a continuous 30Hz, 0.5% L_{ref} peak-to-peak length oscillation was applied to the tissue while it was contracted for 5 min with 10^{-5} M MCh (Fig. S1C). The normalized stiffness was calculated from the peak-to-peak change in stress ($\Delta\sigma$) divided by the strain, or fractional length change. Hysteresivity, a dimensionless quantity that expresses hysteresis as a fraction of the elastic potential energy during an oscillation, was calculated as in (2). In short, when applied to sinusoidal oscillations, η can be calculated as $\eta = \tan(\sin{-1}\ (4A/\pi\Delta F\Delta L))$, with A the area of the force-length loop, ΔF the peak-to-peak force amplitude and ΔL the peak-to-peak length amplitude.

Mass Spectrometry

Ultra-high Liquid Chromatography tandem Mass Spectrometry (uHPLC-MS/MS) was used with the following parameters: After running a single SDS PAGE stacking gel band containing all proteins for each sample, the gel band was reduced, alkylated and digested using trypsin (mass spec sequencing grade, ProMega). Peptides were loaded onto a Thermo Acclaim Pepmap (Thermo, 75uM ID X 2cm C18 3uM beads) precolumn and then onto an Acclaim Pepmap Easyspray analytical column (Thermo, 75uM X

15cm with 2uM C18 beads) separation using a Dionex Ultimate 3000 uHPLC at 220 nl/min with a gradient of 2-35% organic (0.1% formic acid in acetonitrile) over 3 h. Peptides were analyzed using a Thermo Orbitrap Fusion mass spectrometer operating at 120,000 resolution (FWHM in MS1, 15,000 for MS/MS) with HCD sequencing all peptides with a charge of 2+ or greater. The raw data were converted into *.mgf format (Mascot generic format) and searched using Mascot 2.6.2 against Uniprot human sequences. The database search results were loaded onto Scaffold Q+ Scaffold_4.8.9 (Proteome Sciences) for spectral counting. Proteins with an average exclusive peptide count across subjects below 2 were excluded. To isolate differences in the smooth muscle of the whole airway samples, each protein was checked against its prevalence in smooth muscle and non smooth muscle tissues of the airways (cartilage tissue, epithelium, adipocytes, fibroblasts and pneumocytes) as listed in The Protein Atlas (3). Only those proteins which were listed as “not detected” in the non smooth muscle cells and tissues, or were listed as “low” in non smooth muscle tissues and “high” in smooth muscle tissues, were used. To correct for smooth muscle content differences between subjects, we calculated the relative total exclusive spectrum counts (i.e. the mean per protein normalized to 1) for each smooth muscle protein and normalized these by the sum of all the relative spectrum counts of smooth muscle proteins.

Supplementary Figures and Tables

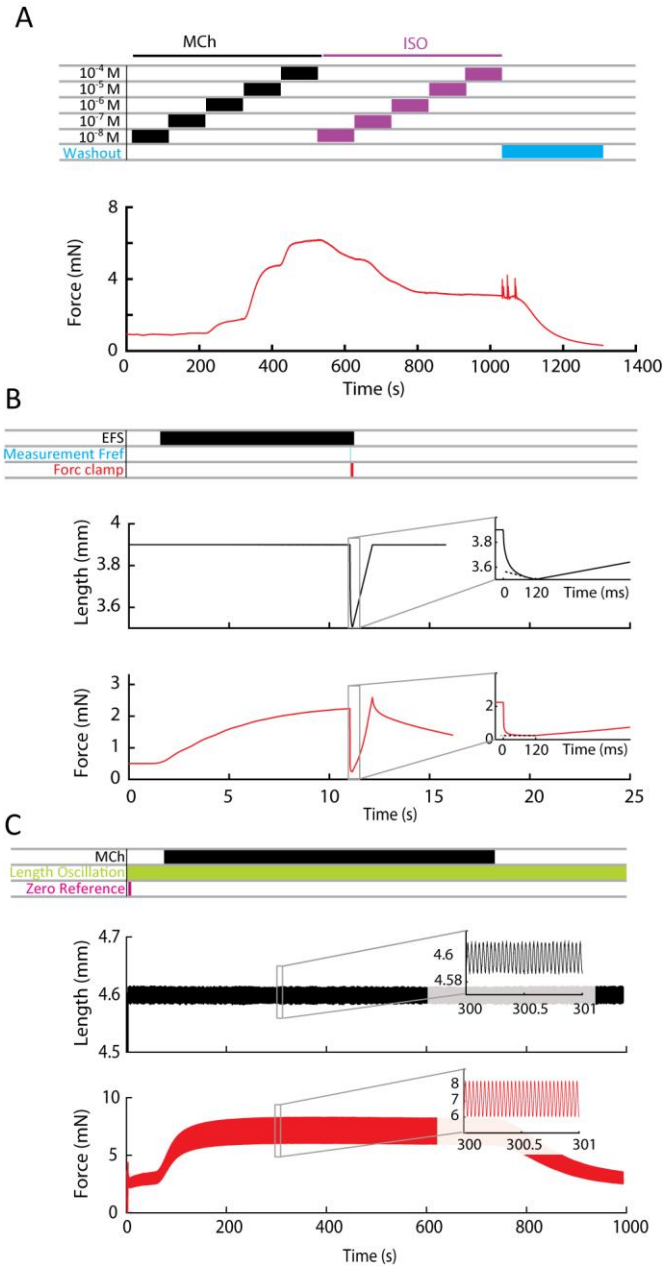

Figure S1: Traces of airway smooth muscle (ASM) mechanics experiments. (A) Sample trace of methacholine (MCh) and isoproterenol (Iso) dose responses. (B) Sample trace of a single EFS force clamp protocol. Top inset shows detail of length during a force clamp, with the slope of the dashed line indicating the shortening velocity. Bottom inset shows detail of force during a force clamp, with force maintained at 5% of the reference force (F_{ref}) for 120ms. (C) Sample trace of length and force oscillations for stiffness and hysteresivity estimation. Insets show detail of length (top) and force (bottom) oscillations.

Table S1: Definition of Abbreviations: A=African American; W=White; H=Hispanic; CVA=Cerebrovascular Accident; HT=Head Trauma; ICH=Intracerebral Hemorrhage; SIGSW=Self Inflicted Gunshot Wound; YA=Years Ago; P.Y.=Per Year. Mechanics Data indicate which experiments were performed on tissue from subject: T=Trachea ASM, IB=Intrapulmonary bronchi ASM, MCh=Methacholine Dose response, Iso=Isoproterenol Dose Response, EFS10=EFS force velocity at 10s, EFS5, 8, 10= EFS force velocity at 5, 8 and 10s, Prot=Proteomics data. *=maximum stress was determined.

Subj.	Sex	Age	BMI	Ethn.	Cause of Death	Asthma history	Other	Medication(s)	Medication in hospital	Data
Asthmatic patients										
1	M	72	44	W	CVA	Age of diagnosis unknown	Smoking 16 P.Y., quit 50 Y.A.			MCh-T*; EFS10-T
2	F	34	32	W	Anoxia from drug intoxication	Diagnosed 20 Y.A., hospitalised twice with exacerbations		Inhaler-Prednisone	Methylprednisolone; Norepinephrine;	MCh-T*
3	M	29	31	W	Anoxia cardiovascular event	Diagnosed 7 years ago	Chewing tobacco for 1 year	Albuterol-Inhaler	Esmolol; Norepinephrine	MCh-T*; EFS10-T
4	M	35	29	W	Anoxia, cardiovascular event	Asthma since childhood.		Albuterol, Budesonide	Norepinephrine; Methylprednisolone; Albuterol	MCh-T*; EFS10-T-IB
5	M	40	27	A	Anoxia, cardiovascular event	Asthma Diagnosed 5 Y.A.		Mometasone and formoterol	Norepinephrine; Methylprednisolone	MCh-T; EFS10-T
6	F	38	36	W	Anoxia cardiovascular event	Asthma diagnosed at 8		Montelukast	Norepinephrine; Epinephrine; Dopamine;	MCh-T-IB; EFS10-T-IB
7	M	23	17	H	CVA	Asthma, unknown when diagnosed	Smoking 7 P.Y. Oxycodone-paracetamol abuse, marijuana & cocaine 1 year	Albuterol	Phenylephrine; Methylprednisolone	MCh-T-IB*; EFS5810-T-IB; Prot
8	F	53	20	W	CVA	Asthma, unknown when diagnosed	Seizure 15 Y.A. , illicit drug use (non IV) 25 Y.A.	Albuterol	Norepinephrine; Epinephrine; Dopamine; Methylprednisolone	MCh-T*-IB*; Iso-T-IB; EFS5810-T-IB; Prot
9	M	23	24	A	Anoxia (Asthma)	Asthma diagnosed age 10, seasonal allergies	Smoking 6 P.Y.	Asthma inhaler (unspecified)	Methylprednisolone, Albuterol	MCh-T*-IB*; Iso-T-IB; EFS5810-T-IB; Prot
10	F	41	24	H	CVA	Asthma, unknown when diagnosed	Hypothyroidism	Asthma medication unknown	Phenylephrine, Vasopressin, Epinephrine, Norepinephrine	MCh-T*-IB*; Iso-T-IB, EFS5810-IB; Prot
11	M	27	26	H	Anoxia, cardiovascular event	Asthma, unknown when diagnosed		Steroid	Norepinephrine, Methylprednisolone, Albuterol	MCh-T*-IB*; Iso-T-IB; EFS5810-T-IB; Prot
12	F	52	33	A	Anoxia, cardiovascular event	History of asthma, resolved but recently	Multiple allergies, diabetes,	Metformin, HTN medications, hemodialysis	Lorezapam; norepinephrine, furosemide;	Prot

						return of symptoms after pneumonia	hypertension, congenital heart disease and heart failure		mannitol	

Control subjects

12	M	22	23	W	Head Trauma 2nd to SIGSW	Asthma as child, not taken medication in 7 years	Smoked Hookah past year	Albuterol as child	Norepinephrine; Phenylephrine; Ipratropium bromide; Albuterol; Methylprednisolone;	MCh-T
13	M	47	26	W	CVA				Phenylephrine	MCh-T*; EFS10-T
14	F	35	22	W	Anoxia from intracranial hemorrhage		Remote marijuana use		Norepinephrine;	MCh-T*; EFS10-T
15	M	30	22	W	Anoxia from Asphyxiation		Smoking: 10 P.Y., Marijuana, Cocaine		Methylprednisolone	MCh-T-IB; EFS10-T-IB; Prot
16	F	54	36	W	CVA		Smoking: 10 P.Y., Quit 8 Y.A.		Epinephrine;	MCh T; EFS10-T
17	F	62	31	W	CVA		Hypertension, Basal cell carcinoma in nose 3 Y.A.		Dopamine	MCh-T*; EFS10-T
18	M	55	27	W	Head trauma		Marijuana occasionally, alcohol abuse		Phenylephrine; Methylprednisolone	MCh-T*-IB*; EFS10-T-IB
19	M	31	24	W	Anoxia, electrocution		Smoking, quit 10 Y.A.		Esmolol, Albuterol	MCh-IB; EFS10-IB; Prot
20	F	58	34	W	CVA				Phenylephrine; Methylprednisolone	EFS10-T
21	F	54	25	W	Head trauma		Smoking 30 P.Y., quit 16 Y.A.; Hypertension		Norepinephrine; Albuterol	MCh-T*; EFS10-T
22	M	49	25	W	HT 2nd GSW		Alcoholism			MCh-T*-IB*; EFS5810-T-IB
23	M	28	22	W	Anoxia 2nd Asphyxiation		Smoking 5 P.Y., Marijuana		Norepinephrine	EFS5810-T-IB
24	F	33	27	A	Anoxia 2nd Drug Intoxication		Bipolar-Depression, Smoking 5 P.Y. Methadone	Depression medication	Norepinephrine, Methylprednisolone	MCh-T*-IB*; Iso-T-IB, EFS5810-T-IB
25	M	38	31	W	Head trauma				Methylprednisolone	MCh-T*-IB*; Iso-T-IB; EFS5810-T-IB
26	F	63	27	W	CVA		Hyperlipidemia, osteopenia	Zocor, methotrexate, Bovina	N/A	MCh-T*-IB*; Iso-T; EFS5810-T-IB
27	F	53	33	W	CVA		Hypertension, anti-phospholipid syndrome, multiple CVA	N/A	Norepinephrine	MCh-T*-IB*; Iso-T-IB; EFS5810-IB; Prot

28	M	18	37	W	Anoxia, cardiovascular event		Autism, Penicillin Allergy	Fluoxetine, Alprazolam, Lisdexamphetamine, Depakote, lithium, Guanfacine, Topiramate, Buspirone, N-Acetyl Cysteine, Prilosec, Clozapine, Clonazepam	Epinephrine, Norepinephrine	MCh-T*-IB*; Iso-T-IB; EFS5810-T-IB; Prot
29	M	55	24	A	CVA		Diabetes, HTN, smoking 40 P.Y., Alcohol 2 per day	Metformin	Methylprednisolone, Epinephrine, Norepinephrine, Heparin, Mannitol, Furosemide, Vasopressin	Prot
30	M	37	37	C	Anoxia, electrocution			none	N/A	Prot

Table S2: Smooth muscle specific proteins

ZYX	Zyxin
PECAM1	Platelet endothelial cell adhesion molecule
SLMAP	Sarcolemmal membrane-associated protein
MYL12A	Myosin regulatory light chain 12A
PTX3	Pentraxin-related protein PTX3
TINAGL1	Tubulointerstitial nephritis antigen-like
SMTN	Smoothelin
VCAN	Versican core protein
SYNPO2	Synaptopodin-2
ACTC1	Actin, alpha cardiac muscle 1
ITGB1	Integrin beta-1
LAMA4	Laminin subunit alpha-4
TPM1	Tropomyosin alpha-1 chain
CNN1	Calponin-1
PALLD	Palladin
MYLK	Myosin light chain kinase, smooth muscle
PGM5	Phosphoglucomutase-like protein 5
TAGLN	Transgelin
DES	Desmin
ACTA2	Actin, aortic smooth muscle
MYH11	Myosin-11o
AEBP1	Adipocyte enhancer-binding protein 1
SRPRB	Signal recognition particle receptor subunit beta
THBS1	Thrombospondin-1
CALD1	Caldesmon
ACTB	Actin, cytoplasmic 1
FLNA	Filamin-A

Table S3: Significantly altered proteins in total airway extract

KANK2	KN motif and ankyrin repeat domain-containing protein 2
SYNM	Synemin
SORBS1	Sorbin and SH3 domain-containing protein 1
SMTN	Smoothelin
LPP	Lipoma-preferred partner
MCAM	Cell surface glycoprotein MUC18
FLNC	Filamin-C
BASP1	Brain acid soluble protein 1
GPX3	Glutathione peroxidase 3
COL4A2	Collagen alpha-2(IV) chain
SYNPO2	Synaptopodin-2
PGM5	Phosphoglucomutase-like protein 5
PALLD	Palladin
POSTN	Periostin
NID1	Nidogen-1
MYL9	Myosin regulatory light polypeptide 9
NDUFA9	NADH dehydrogenase [ubiquinone] 1 alpha subcomplex subunit 9, mitochondrial
FERMT2	Fermitin family homolog 2
CORO1C	Coronin-1C
SUN2	SUN domain-containing protein 2
MYH11	Myosin-11o
MYLK	Myosin light chain kinase, smooth muscle
CYC1	Cytochrome c1, heme protein, mitochondrial
ITGB1	Integrin beta-1
CRIP2	Cysteine-rich protein 2
EMILIN1	EMILIN-1
CALD1	Caldesmon
PFKL	ATP-dependent 6-phosphofructokinase, liver type
CAVIN3	Caveolae-associated protein 3
DES	Desmin
CSRP1	Cysteine and glycine-rich protein 1
PGM2	Phosphoglucomutase-2
ATP2B4	Plasma membrane calcium-transporting ATPase 4
LGALS3	Galectin-3
ILK	Integrin-linked protein kinase
LAMA5	Laminin subunit alpha-5
LAMB2	Laminin subunit beta-2
TNS1	Tensin-1
FLNA	Filamin-A
RAB10	Ras-related protein Rab-10
DSTN	Destrin
HSPG2	Basement membrane-specific heparan sulfate proteoglycan core protein
CLIC4	Chloride intracellular channel protein 4
CHCHD3	MICOS complex subunit MIC19
RSU1	Ras suppressor protein 1
VCL	Vinculin
AOC3	Membrane primary amine oxidase
AIFM1	Apoptosis-inducing factor 1, mitochondrial
TLN1	Talin-1

CAVIN1	Caveolae-associated protein 1
H1F0	Histone H1.0
RAP1B	Ras-related protein Rap-1b
WDR1	WD repeat-containing protein 1
EHD2	EH domain-containing protein 2
CAND1	Cullin-associated NEDD8-dissociated protein 1
ACTA2	Actin, aortic smooth muscle
MYO1C	Unconventional myosin-Ic
DPYSL3	Dihydropyrimidinase-related protein 3
RPS27A	Ubiquitin-40S ribosomal protein S27a
SRI	Sorcin
H2AFY	Core histone macro-H2A.1
SERPINB6	Serpin B6
DLD	Dihydrolipoyl dehydrogenase, mitochondrial
UQCRC2	Cytochrome b-c1 complex subunit 2, mitochondrial
DLST	Dihydrolipoyllysine-residue succinyltransferase component of 2-oxoglutarate dehydrogenase complex, mitochondrial
HMGB1	High mobility group protein B1

Table S4: Database for Annotation, Visualization and Integrated Discovery (DAVID) gene ontology cell component enrichment.

Gene Ontology Term	Count	Bonferroni
GO:0005856 cytoskeleton	26	1.61E-04
→ GO:000015629 actin cytoskeleton	17	7.59E-05
GO:0030054 cell junction	10	0.015271
→ GO:0070161 anchoring junction	10	0.001082
→ GO:0005912 adherens junction	10	0.001082
→ GO:0005924 cell-substrate adherens junction	9	6.60E-04
→ GO:0005925 focal adhesion	8	0.005607
→ GO:0030055 cell-substrate junction	9	9.97E-04
→ GO:0005924 cell-substrate adherens junction	9	6.60E-04
→ GO:0005925 focal adhesion	8	0.005607
GO:0043292 contractile fiber	10	0.005995
→ GO:0044449 contractile fiber part	10	0.004638
GO:0016323 basolateral plasma membrane	10	0.009736

Count column shows the number of proteins that were enriched within this term, out of 66 proteins that were enriched in subjects with asthma. The Bonferroni column shows the Bonferroni corrected p-value of the enrichment. Grey lines indicate duplicate gene ontology terms that appear in multiple hierarchies.

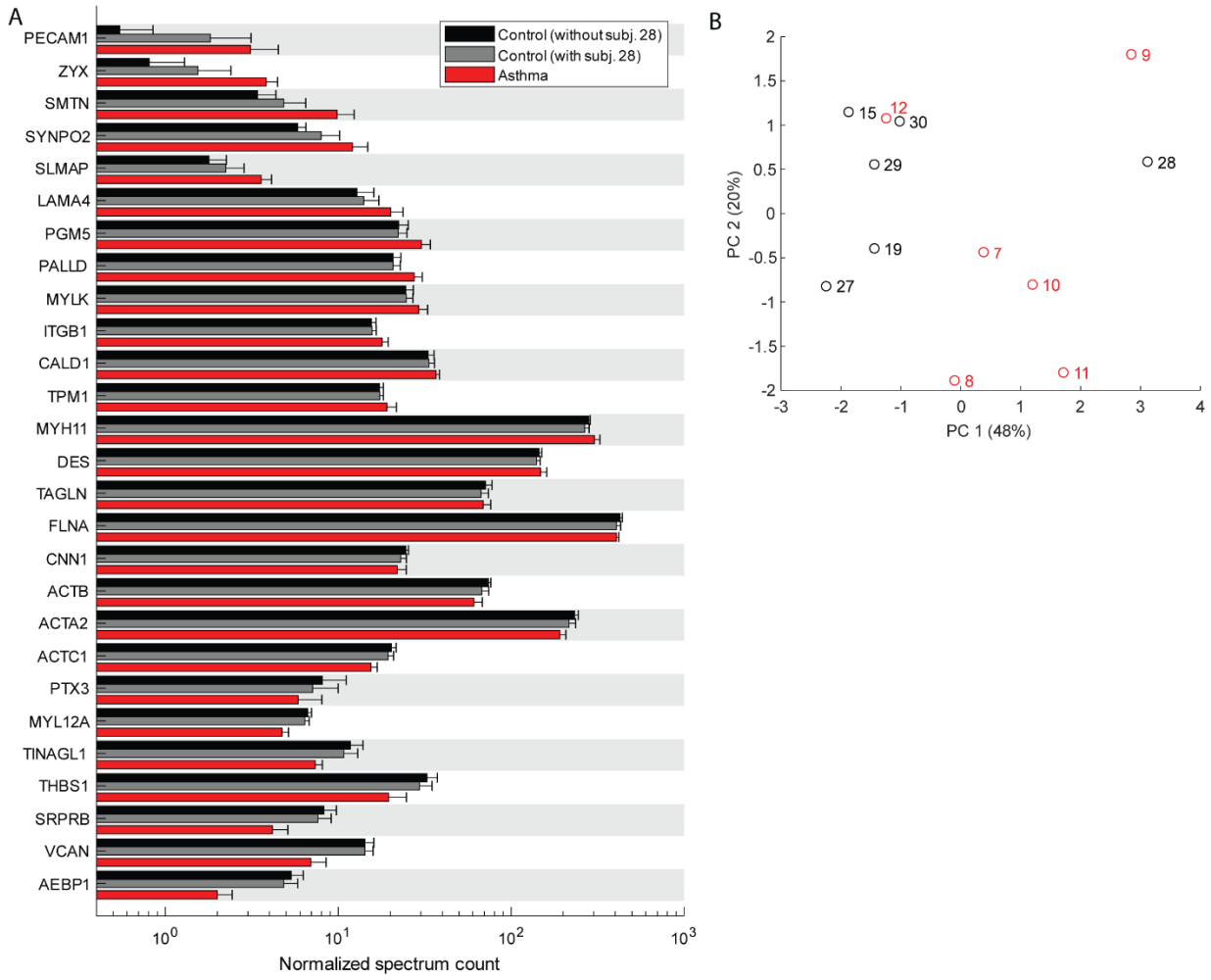

Figure S2 Proteomics data from airway smooth muscle (ASM) specific proteins. (A) Normalized spectrum counts for all smooth muscle specific proteins with a minimum average spectrum count of 2. Black bars are all control subjects excluding clinical outlier subject 28. Grey bars are all control subjects. Red bars are all subjects with asthma. (B) PCA for smooth muscle specific proteins. Black circles are control (subject numbers between brackets) and red circles are asthmatics.

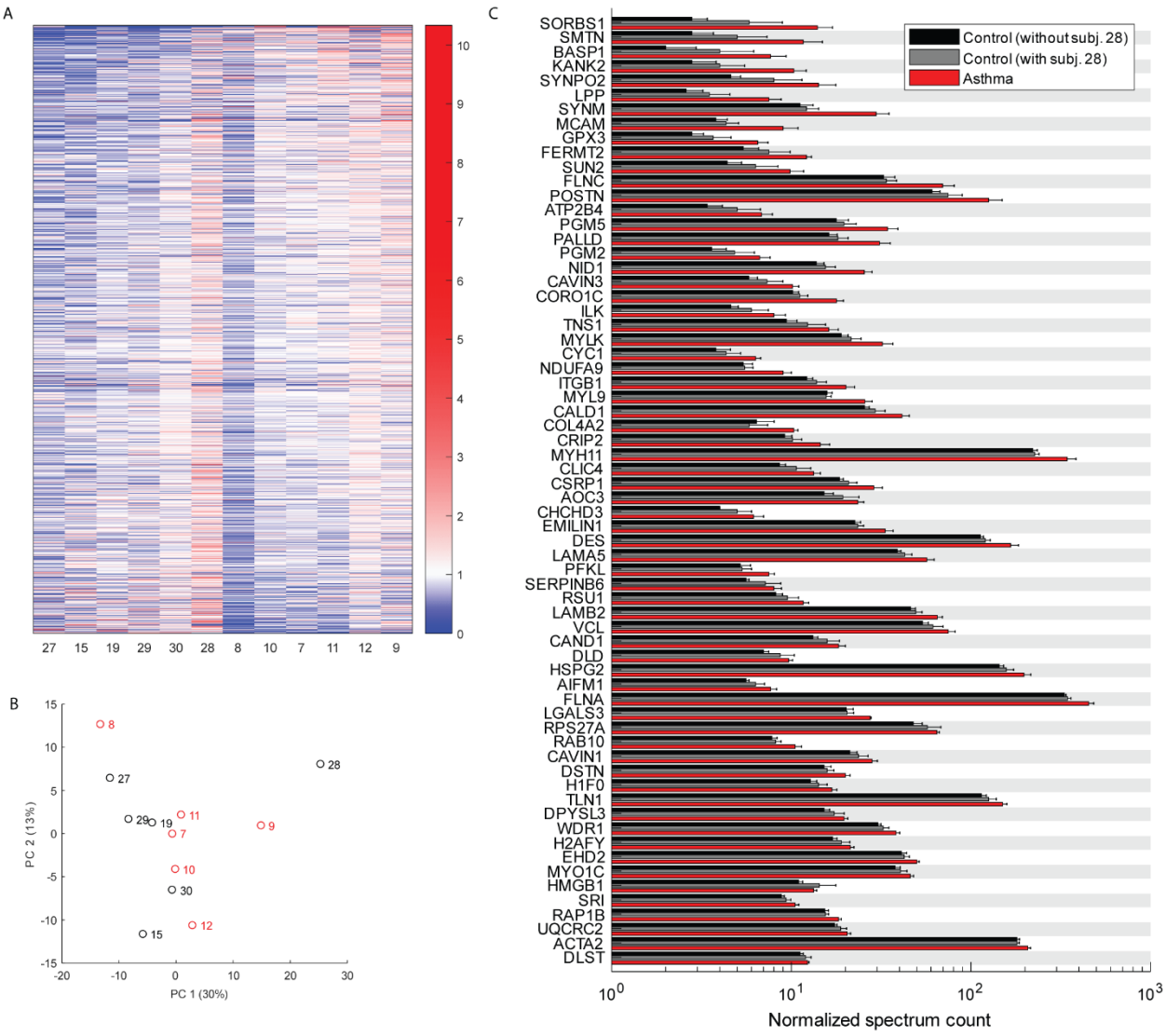

Figure S3: Proteomics data for whole airway extracts. (A) Heatmap of all proteins detected. Subject numbers as in Table 1 (B) PCA for all proteins and all subjects. Black circles are control (subject numbers between brackets) and red circles are asthmatics. (C) Normalized spectrum counts for the 66 proteins that are significantly different in subjects with asthma ($p<0.05$ without correction for multiple comparison). Black bars are all control subjects excluding clinical outlier subject 28. Grey bars are all control subjects. Red bars are all subjects with asthma.

References

1. Bullimore SR, Saunders TJ, Herzog W, & MacIntosh BR (2010) Calculation of muscle maximal shortening velocity by extrapolation of the force–velocity relationship: afterloaded versus isotonic release contractions. *Can. J. Physiol. Pharmacol.* 88(10):937-948.
2. Fredberg JJ*, et al.* (1997) Airway smooth muscle, tidal stretches, and dynamically determined contractile states. *Am J Respir Crit Care Med* 156(6):1752-1759.
3. Uhlén M*, et al.* (2015) Tissue-based map of the human proteome. *Science* 347(6220):1260419.
4. Ammit AJ, Armour CL, & Black JL (2000) Smooth-Muscle Myosin Light-Chain Kinase Content Is Increased in Human Sensitized Airways. *Am J Respir Crit Care Med* 161(1):257-263.
5. Walsh MP*, et al.* (2011) Rho-associated kinase plays a role in rabbit urethral smooth muscle contraction, but not via enhanced myosin light chain phosphorylation. *American Journal of Physiology-Renal Physiology* 300(1):F73-F85.